

Linear and dynamical photoinduced dichroisms of InAs/GaAs self-assembled quantum dots: Population relaxation and decoherence measurements

F. Bernardot, E. Aubry, J. Tribollet, C. Testelin, and M. Chamarro

Institut des NanoSciences de Paris, Universités Paris VI-VII, CNRS UMR 7588, 140 rue de Lourmel, 75015 Paris, France

L. Lombez, P.-F. Braun, X. Marie, and T. Amand

Laboratoire de Nanophysique, Magnétisme et Optoélectronique, INSA, 135 avenue de Rangueil, 31077 Toulouse Cedex 4, France

J.-M. Gérard

Nanophysics and Semiconductors Laboratory, CEA/DRFMC/SP2M, 17 rue des Martyrs, 38054 Grenoble Cedex, France

(Received 29 July 2005; revised manuscript received 9 November 2005; published 1 February 2006)

We present and model our pump-probe experiments measuring the photoinduced dynamics of an ensemble of self-assembled InAs/GaAs quantum dots. A pulsed pump beam, linearly polarized along an in-plane symmetry axis of the quantum dots, photoinduces a linear dichroism. We show that the dynamics of this linear dichroism is consistent with a long spin relaxation time and allows us to measure different radiative lifetimes for both nondegenerate, low-lying, electron-hole pair states. In another experimental configuration, when the pump beam creates a coherent superposition of these electron-hole pair states, it photoinduces a dynamical dichroism, which gives information about quantum decoherence and provides the electron-hole anisotropic exchange interaction energy splitting, $41 \pm 8 \mu\text{eV}$ at 1.343 eV. A model is developed, which accounts for the dynamical dichroism and predicts the experimental observations with good accuracy.

DOI: [10.1103/PhysRevB.73.085301](https://doi.org/10.1103/PhysRevB.73.085301)

PACS number(s): 78.67.Hc, 78.66.Fd, 78.47.+p

I. INTRODUCTION

The atomlike properties of semiconductor quantum dots¹ (QDs) make these nanostructured materials very attractive candidates for use in many quantum devices, such as single-electron devices,² detectors,³ single-photon sources,^{4,5} and solid-state quantum logic gates.^{6,7} In this context, it is of prime importance to have detailed knowledge of the electronic structure of the low-lying electron-hole ($e-h$) pair states (often called “exciton ground states”) and also of the characteristic times of their population relaxation and quantum decoherence.

In recent years, progress in single-QD photoluminescence (PL) experiments revealed the loss of the nominal rotational symmetry of the low-lying $e-h$ pair states of self-assembled QDs. The micro-PL technique showed a fine-structure doublet for the lowest-excited $e-h$ pair states, exhibiting a pronounced in-plane polarization anisotropy^{8–10} which singularizes the seemingly equivalent $[1\bar{1}0]$ and $[110]$ directions. Indeed, due to this symmetry lowering (induced by a shape anisotropy and/or by the anisotropy between the $[1\bar{1}0]$ and $[110]$ directions in the zinc-blende crystal structure), the degeneracy between the two bright states is lifted by the long-range exchange interaction and the oscillator strengths of these two nondegenerate states become different.¹¹ The experimental determination of the value of this splitting (on the order of several tens of μeV) has been the center of recent studies based on differential transmission,^{12,13} transient four-wave mixing,¹⁴ or PL.^{15,16}

Time-resolved PL experiments are largely used to obtain information about population lifetimes. Recently, the low-temperature PL of QDs has shown a remarkable memory of the polarization of the exciting light, which demonstrates an

inefficient transfer mechanism between both $e-h$ pair states. To have access to their decoherence time, it is, however, necessary to experimentally create a coherent superposition of the $e-h$ pair states and to measure their relative phase. That is possible in differential transmission,¹⁷ four-wave mixing,¹⁸ and PL measurements.^{15,16}

In this paper, we present and model our pump-probe experiments, in which we measure the photoinduced dynamics of an ensemble of InAs/GaAs QDs. Our model treats the pump-QD interaction exactly, while the weak probe beam is supposed to negligibly perturb the excited sample. Our measurements allow us to get information not only about the fine structure of the $e-h$ pair states, but also about their population lifetime and decoherence time. In particular, we have obtained an energy splitting of the low-lying $e-h$ states equal to $41 \pm 8 \mu\text{eV}$, at 1.343 eV, and have observed two different radiative lifetimes for these states.

II. SAMPLE AND EXPERIMENTAL SETUP

The sample studied is made of 40 layers of self-assembled InAs/GaAs QDs grown by molecular beam epitaxy. The mean density of the QDs is $N=4 \times 10^{10} \text{ cm}^{-2}$ per layer, with a typical dot height of 5 nm and a diameter of 15 nm. The PL spectrum at 2 K shows a maximum at 1.34 eV and a full width at half maximum of about 60 meV.¹⁹

We use different beam-polarization configurations of our pump-probe experimental setup in order to obtain information on the electronic structure of the low-lying $e-h$ pair states and on the dynamics of their relaxation and decoherence. Pump and probe pulses have a duration of 2 ps and are supplied by a mode-locked Ti:sapphire laser with a repetition rate of 76 MHz. The average intensity of the pump is about

1 W/cm² and typically 10 times larger than the probe intensity. Both beams are quasicollinearly focused onto the sample placed inside a cryostat. Measurements are performed at 2 K. After transmission through the sample, a balanced optical bridge decomposes and analyzes the probe beam into two linear components: aligned with the directions $[1\bar{1}0]$ and $[110]$ of the eigenaxes of the InAs/GaAs QDs for linear dichroism measurements and aligned with the $[100]$ and $[010]$ axes for dynamical dichroism experiments. The difference in the intensity of these two transmitted components is finally measured. Intensity modulations of the pump and probe beams are used to improve the signal-to-noise ratio.^{19,20}

We have also performed circular dichroism experiments in order to check the possible presence of charged QDs in our nonintentionally doped sample. Indeed, this experimental configuration is especially well adapted to evidence charged QDs, because their eigenstates are circularly polarized. No signal of circular dichroism during the e - h pair lifetime was detected, leading to the assumption of a wholly undoped sample.

III. PUMP-PROBE EXPERIMENTS: MODEL

In this paper we model our pump-probe experiments, in which the photoinduced dynamics of an ensemble of InAs/GaAs QDs is measured. For simplicity, we describe the interaction of light with a sample containing a single layer of independent QDs. The pump or probe optical beam is approximated by a plane wave propagating along the growth axis z of the sample. Aligned along the in-plane $[110]$ and $[1\bar{1}0]$ crystallographic directions, the linear x and y light components couple the ground state $|g\rangle$ to the $|x\rangle$ and $|y\rangle$ e - h pair states through Π_x and Π_y transitions, respectively. The $|x\rangle$ and $|y\rangle$ e - h pair states are ± 1 spin states along the x axis: $|x\rangle = |J_x = +1\rangle = (|+\rangle + |-\rangle)/\sqrt{2}$ and $|y\rangle = |J_x = -1\rangle = (|+\rangle - |-\rangle)/i\sqrt{2}$, where the $|\pm\rangle = |J_z = \pm 1\rangle$ are the states coupled to the ground state through σ_{\pm} transitions when no anisotropy is present. The energy level schema is V shaped (see Fig. 1), with both e - h pair states lying an energy $\hbar\omega_0$ above the ground state and separated by the e - h anisotropic exchange energy splitting $\hbar\delta_1$. The interaction with light of a single QD located in the $z=0$ plane is described by a dipolar interaction, whose Hamiltonian in the rotating-wave approximation is written

$$H_I(t) = - \sum_j d_j E_j e^{-i\omega t} |j\rangle \langle g| + \text{H.c.}, \quad (1)$$

where d_j is the dipole on the transition $|g\rangle/|j\rangle$ and E_j the j component of the optical-field envelope ($j=x,y$). Linking the ‘‘A.P’’ and ‘‘E.D’’ descriptions of $H_I(t)$,²¹ one obtains $d_j = -ep_j/im_e\omega$, where p_j is the j component of the linear-momentum matrix element between $|g\rangle$ and $|j\rangle$. Using the envelope-function approximation to describe the states $|g\rangle$, $|x\rangle$, and $|y\rangle$ and the value²² $p_j = 1.27 \times 10^{-24}$ SI in InAs for the linear-momentum matrix element between both Bloch functions of an e - h pair, we estimate $d_j = 1.1 \times 10^{-28}$ C m—assuming a perfect overlap of the electron and

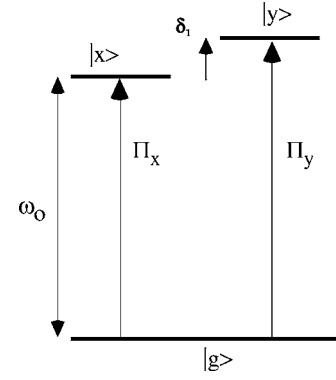


FIG. 1. Lowest-energy states in a quantum dot. $|g\rangle$ is the ground state (filled valence band, empty conduction band). The $|x\rangle$ ($|y\rangle$) electron-hole pair state is resonantly excited from $|g\rangle$ through a linearly polarized optical transition Π_x (Π_y) of frequency ω_0 ($\omega_0 + \delta_1$).

hole envelope functions.²³ This electric dipole corresponds to two elementary opposite charges $\pm e$ separated by 0.7 nm.

The duration $\tau_p = 2$ ps of the optical pulses being very short as compared to $1/|\omega - \omega_0|$, light is supposed to be resonant with both linear transitions of a QD; this condition means that the Π_y transition is resonant as well, because $\tau_p \ll 1/|\delta_1|$ is also expected. The envelopes $E_j(t)$ of the pump-field components have a slowly varying profile and have maximum amplitudes E_{0j} . We assume that there is no relaxation in the QDs during the interaction of a pump or probe pulse with the sample; in particular, a single QD interacting with a pump pulse is well described by a pure quantum state. The solution of the time-dependent Schrödinger equation takes the following expression, immediately after the pump pulse (centered at $t=0$):

$$|\Psi(t)\rangle = \cos \Omega_0 \tau |g\rangle + i \sin \Omega_0 \tau e^{-i\omega_0 t} \times \{ \Omega_{0x} |x\rangle + e^{-i\delta_1 t} \Omega_{0y} |y\rangle \} / \Omega_0, \quad (2)$$

where τ is the time integral of the normalized pulse profile and the complex Rabi frequencies $\Omega_{0j} = d_j E_{0j} / \hbar$ ($j=x,y$) characterize the coupling of the pump field with the Π_x and Π_y linear transitions of the QD ($\Omega_0 = [|\Omega_{0x}|^2 + |\Omega_{0y}|^2]^{1/2}$). Equation (2) generalizes the well-known formula concerning a two-level system which interacts with a classical field;²⁴ it shows that the optical coherence of the pump pulse between its x and y components—this coherence being marked by the relative weight $|E_{0y}|/|E_{0x}|$ and the relative phase $\text{Arg}(E_{0y}/E_{0x})$ —is transferred to the e - h pair part of the QD state $|\Psi(t)\rangle$ immediately after the pump pulse has passed, with slight modifications brought by the QD itself ($d_x \neq d_y$, $\delta_1 \neq 0$).

After their interaction with the pump pulse and before the probe pulse arrives, the QDs freely evolve. To describe the quantum state of a QD in presence of relaxation, we turn to a density matrix formalism. Immediately after the pump pulse, the density matrix of a single QD is $\rho(t) = |\Psi(t)\rangle \langle \Psi(t)|$. Afterwards, the populations of $|x\rangle$ and $|y\rangle$ relax to the ground state $|g\rangle$, with rates $1/\tau_x$ and $1/\tau_y$, respectively; the lifetimes τ_x and τ_y are *a priori* different, in accor-

dance with $d_x \neq d_y$. Taking into account previous studies^{15,25} of resonant PL of the first-excited e - h pair states in our sample, we consider that, at the nanosecond time scale of our experiments, the spin relaxation between the $|x\rangle$ and $|y\rangle$ states via a spin-flip mechanism is nearly absent in our InAs QDs, and we neglect it completely. Dark states, with total angular momentum $J=2$, are not considered because recent studies on similar undoped InAs QDs have shown a very long low-temperature spin-flip time between dark and bright states [from 30 ns to 400 ns (Refs. 26 and 27)]. The populations of the e - h pair states are then written

$$\rho_j(t) = (|\Omega_{0j}|^2/\Omega_0^2)\sin^2 \Omega_0 \tau \exp\{-t/\tau_j\}, \quad (3)$$

$j=x$ or y . Concerning the coherences, $\rho_{xg}(t)$ and $\rho_{yg}(t)$ are possibly long lived;²⁸ nevertheless, they cannot be measured in our experiments, and we do not consider them further. On the contrary, we are able to measure the coherence $\rho_{yx}(t)$ between the e - h pair states $|x\rangle$ and $|y\rangle$; noting T_2 , its characteristic damping time, and using Eq. (2), we write

$$\rho_{yx}(t) = (\Omega_{0y}\Omega_{0x}^*/\Omega_0^2)\sin^2 \Omega_0 \tau e^{-i\delta_1 t} \exp\{-t/T_2\}. \quad (4)$$

Note that Eqs. (3) and (4) concern a single QD.

The populations $\rho_x(t)$ and $\rho_y(t)$ and the coherence $\rho_{yx}(t)$ are the physical quantities we are able to reach in our experiments, in order to characterize the quantum dynamics of the measured QDs. For this purpose, the probe pulse is sent to the out-of-equilibrium sample at a time delayed from the arrival of the pump pulse. As shown in the following, for well-chosen polarization configurations of the pump and probe beams, the detection of the probe pulse after its interaction with the QDs reveals their (averaged) quantum state when it crossed them. The calculation of the measured signal on the probe is achieved in two steps (cf. Appendix A). First, the effect of the probe pulse on the density matrix of a QD is evaluated to linear order in the probe optical field. Second, the classical optical radiation of the QDs is added to the probe field after it has crossed the plane of QDs, in a procedure which do not necessitate a field quantization.²⁹ Finally, taking into account the peculiarities of our polarization-sensitive detection, we can write down formulas corresponding to various polarization configurations for the pump and probe beams. As experimentally demonstrated, appropriate choices of polarizations for the pump and probe beams do allow to reach all the quantities of interest concerning the QDs—namely the populations $\rho_x(\Delta t)$ and $\rho_y(\Delta t)$ of both e - h pair states and the coherence $\rho_{yx}(\Delta t)$ between them—at various delay times Δt between the pump and probe pulses. From these, we deduce the lifetimes τ_x and τ_y , the ratio of the oscillator strengths d_x^2 and d_y^2 and the fine-structure splitting δ_1 .

IV. PHOTOINDUCED LINEAR DICHROISM EXPERIMENTS

We first consider the experimental configurations in which the pump pulse is linearly polarized along the x axis, $E_y=0$, or along the y axis, $E_x=0$. In these cases, $\Omega_{0y}=0$ or $\Omega_{0x}=0$; then, no coherence can exist between the e - h pair states:

$\rho_{yx}(\Delta t)=0$. Thus, the eigenpropagation modes for the probe are linearly polarized along the x and y axes, at any time, and the envelope of the probe field after crossing the layer of QDs has the components

$$e_{0j} \left\{ p(t - nz/c - \Delta t) - [\rho_g(\Delta t) - \rho_j(\Delta t)] d_j^2 Z(N\omega/2\hbar) \times \int_{-\infty}^{t-nz/c} dt' p(t' - \Delta t) \right\}, \quad j=x \text{ or } y, \quad (5)$$

where $p(t)$ is the normalized profile of the optical pulses (n is the GaAs index of refraction and Z its electromagnetic impedance). After the layer of QDs, the modulus of the x component of the probe field is diminished by an amount proportional to $[\rho_g(\Delta t) - \rho_x(\Delta t)] d_x^2$. The $\rho_g(\Delta t)$ contribution is the absorption decrease due to the depletion of the ground state; the $\rho_x(\Delta t)$ contribution is the stimulated emission on the Π_x transition originating from the population already existing in the $|x\rangle$ state when the resonant probe crosses the sample. Both preceding processes are proportional to the oscillator strength d_x^2 . The same discussion is valid as well for the y component of the probe. This means that a Π_x or Π_y pump pulse modifies the linear dichroism along the x and y eigenaxes, which exists in the layer of QDs in the absence of a pump beam, then creating a photoinduced linear dichroism.

Experimentally, the mean optical intensities I_x and I_y of the x and y probe components after the sample are measured by a quadratic detector, whose response time is much larger than the duration $\tau_p=2$ ps of the pulses. The incident probe beam has a linear polarization oriented at nearly 45° to the x and y axes, in such a way that I_x and I_y are equal in the absence of a pump pulse. Under this condition, the pump-induced experimental signal when the pump beam is Π_x or Π_y polarized is found to be

$$I_x - I_y \propto d_x^2 \{ [1 - \rho_g(\Delta t)] + \rho_x(\Delta t) \} - d_y^2 \{ [1 - \rho_g(\Delta t)] + \rho_y(\Delta t) \}. \quad (6)$$

This expression makes clear that the population disequilibrium on the transition Π_x (Π_y) is felt by the probe pulse through the oscillator strength d_x^2 (d_y^2) of this transition. For a Π_x pump beam, $\rho_y(\Delta t)=0$, and the signal is written

$$I_x - I_y \propto (2 - r) \sin^2 |\Omega_{0x}| \tau \exp\{-\Delta t/\tau_x\}, \quad (7a)$$

where $r=d_y^2/d_x^2$ is the ratio of the oscillator strengths. When the pump polarization is turned to Π_y , the signal becomes

$$I_x - I_y \propto -(2r - 1) \sin^2 |\Omega_{0y}| \tau \exp\{-\Delta t/\tau_y\}. \quad (7b)$$

Figure 2 shows the measured linear dichroism decay curves observed at low temperature for a pump and probe beam energy of 1.343 eV. The upper curve corresponds to a pump linearly polarized along the vertical direction with respect to the experimental setup, and the lower one corresponds to a pump linearly polarized along the horizontal direction. Horizontal and vertical directions are parallel to the two crystallographic axes $[1\bar{1}0]$ and $[110]$. Both decays are nonsymmetric with respect to the zero line, both in amplitude and in characteristic damping time; that is a conse-

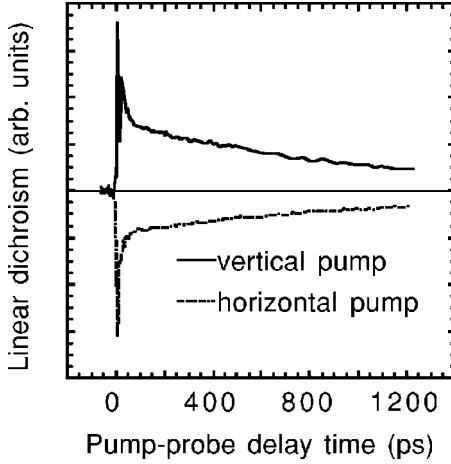


FIG. 2. Linear dichroism, at 2 K, as a function of the pump-probe delay, for a pump and probe energy of 1.343 eV. The solid (dotted) line represents experimental data for a vertically (horizontally) polarized pump beam.

quence of the difference in the oscillator strengths for the Π_x and Π_y transitions. Using the semilogarithmic plot of Fig. 3, we measure a very short decay time of 20 ps and a longer one in the nanosecond scale. One possible explanation for this two-exponential decay is that, at a given energy, the pump beam is able to excite two different assemblies of QDs: one assembly of large-sized QDs, excited in the second-excited states of the e - h pair, and a second assembly of small-sized QDs, excited in the first-excited e - h pair states. The shorter characteristic time obtained from the two-exponential decay curves of Fig. 3 represents the lifetime of the second-excited states to the first-excited states or to the ground state in the largest QDs.³⁰ The long-time decay is associated to the resonant excitation of the $|x\rangle$ or $|y\rangle$ states in small QDs, which is the studied situation.

Fits of the long-time decays of Fig. 3 with Eqs. (7) give $\tau_V = 1038 \pm 18$ ps and $\tau_H = 1164 \pm 36$ ps, which leads to an os-

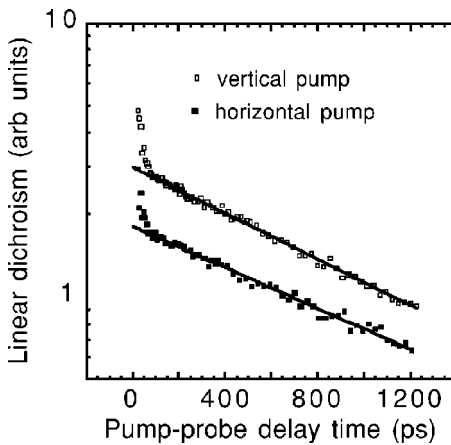


FIG. 3. Semilogarithmic plot of Fig. 2, for positive pump-probe delays. The open (solid) squares represent the experimental data for a vertically (horizontally) polarized pump beam. The straight lines are one-exponential decay fits, for the long-time signals; two different decays are measured, $\tau_V = 1038 \pm 18$ ps and $\tau_H = 1164 \pm 36$ ps, which are consistent with the relative amplitudes of the curves.

cillator strengths ratio $r = 0.89 \pm 0.04$, according to the Fermi golden rule $\tau^{-1} \propto d^2$. These mean decay times are in good agreement with time-resolved PL experiments on this sample, which have demonstrated an e - h pair radiative decay of about 1 ns, at 1.33 eV.¹⁵ Moreover, as we estimate $|\Omega_{0j}|\tau$ to be less than 0.5 rad, we replace $\sin^2|\Omega_{0j}|\tau$ by $(|\Omega_{0j}|\tau)^2$ in Eqs. (7), which implies a small error of the order of 1% when manipulating the ratio of these equations; then, from the extrapolated long-time signal amplitudes to $\Delta t = 0$ of the upper and lower curves of Fig. 2, we obtain an oscillator strengths ratio $r = 0.88 \pm 0.02$: the relative amplitudes of both curves of Fig. 2 are in complete agreement with their relative decay times.

Let us comment on the absence of the biexciton state in our analysis. It is possible for the biexciton transition to be resonant in our experiment—i.e., its binding energy to be within the 1 meV width of the laser energy; nevertheless, the following reasons indicate that the biexciton state is negligible. First, our pump intensity is too weak to create a resonant biexciton with a non-negligible probability. Second, if we assume that the probe transmission is sensitive to a resonant biexciton transition, then the linear dichroism, given in Eqs. (7), is affected only in its amplitudes at $\Delta t = 0$, but not in its temporal behavior: the fact that the initial amplitudes are consistent with the damping rates, in the framework of our model, is a strong indication that the biexciton state plays a negligible role in our experiment.

V. DYNAMICAL DICHROISM EXPERIMENTS

When the pump pulse is not linearly polarized along the x or y eigenaxis, some coherence builds up between the $|x\rangle$ and $|y\rangle$ e - h pair states, in addition to the induced modification of their populations. At the time $t = \Delta t$ when the probe pulse impinges the sample, one can hope that this $|x\rangle/|y\rangle$ coherence is still present, $\rho_{yx}(\Delta t) \neq 0$. The full expression of $\bar{\sigma}_{jg}(t) - \bar{\rho}_{jg}(\Delta t)$, Eqs. (A3), then needs to enter in the field $\tilde{\mathcal{E}}_j(z > 0, t)$ radiated by the layer of QDs as the probe crosses it ($j = x$ or y), Eqs. (A6). Experimentally, we use an incident probe beam linearly polarized along the x axis; the measured signal is the optical intensity difference in the two orthogonal components which are at $\pm 45^\circ$ to the incident polarization. Under these conditions, the signal is written, beside a constant factor,

$$\langle \text{Re}\{e_x(t - nz/c - \Delta t) \tilde{\mathcal{E}}_y(z > 0, t - nz/c)\} \rangle, \quad (8)$$

where $\langle \dots \rangle$ stands for a time averaging and is then proportional to the rotation $\theta(\Delta t)$ undergone by the polarization of the incident x -polarized probe after the sample; more precisely, $\theta(\Delta t)$ is the angle between the x axis and the major axis of the probe polarization after the sample. This angle finally takes the expression

$$\theta(\Delta t) \propto \text{Re}\{\rho_{yx}(\Delta t)\} \propto \text{Re}\{E_{0y}E_{0x}^* e^{-i\delta_1\Delta t}\} \exp\{-\Delta t/T_2^*\}, \quad (9a)$$

where, as a result of the averaging over the QDs, δ_1 is a mean value and T_2^* replaces T_2 (the exponential decay as-

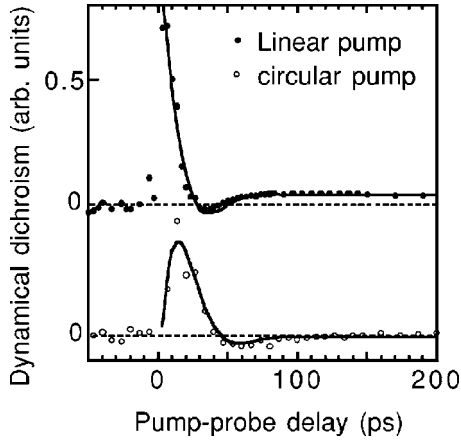


FIG. 4. Dynamical dichroism, at 2 K, as a function of the pump-probe delay, for a pump and probe energy of 1.343 eV. Open (solid) circles represent experimental data for a circular (linear at 45° to the QD eigenaxes) pump; the line represents a fit of the experimental data to a damped sine (cosine) function. From these data, we deduce a mean energy splitting $\hbar\delta_1=41\pm 8\ \mu\text{eV}$ and $T_2^*=16\ \text{ps}$.

sumes a Lorentzian distribution of fine-structure splittings among the QDs, which will be discussed in the following).

For a pump beam linearly polarized at $\pm 45^\circ$ to the x and y axes, $E_{0y}=\pm E_{0x}$ and

$$\theta(\Delta t) \propto \pm \cos(\delta_1 \Delta t) \exp\{-\Delta t/T_2^*\}, \quad (9b)$$

whereas in the case of a circularly polarized pump, $E_{0y}=\pm iE_{0x}$ and

$$\theta(\Delta t) \propto \pm \sin(\delta_1 \Delta t) \exp\{-\Delta t/T_2^*\}. \quad (9c)$$

We can trace the origin of the initial phase for the oscillations of $\theta(\Delta t)$. Considering the case of a circularly polarized pump for example, the y component $\tilde{E}_y \propto \rho_{yx}(\Delta t)$ [cf. Eqs. (A6), (A3b), and (2)] of the QD-radiated field is in quadrature with the x -polarized incident probe at $\Delta t=0$. The field after the sample is then elliptically polarized with a principal axis along x , so that no signal is observed. Afterwards, $\rho_{yx}(\Delta t) \propto \pm i e^{-i\delta_1 \Delta t}$ gains a nonzero real part, the principal axis of the polarization ellipse turns, and the signal begins to exist; later, the signal is maximum at $\Delta t=\pi/2|\delta_1|$ when $\rho_{yx}(\Delta t)$ is purely real, then starts to decrease as $\rho_{yx}(\Delta t)$ is reacquiring a nonzero imaginary part, and so on. For the case of a linear pump polarization at $\pm 45^\circ$ to the x and y axes, the discussion is the same, except for a nonzero signal at $\Delta t=0^+$ arising from a pure real $\rho_{yx}(0^+)$.

These $\theta(\Delta t)$ oscillations arise from the existence of a quantum coherence $\rho_{yx}(\Delta t)$ between the $|x\rangle$ and $|y\rangle$ e - h pair states and thus have no counterpart in classical optics. Appendix B shows that this phenomenon comes from a dichroism between two elliptical eigenpropagation modes in the sample, the eigenpolarizations and associated absorptions varying in time. We are thus facing a *dynamical dichroism*, which exists as long as the $|x\rangle/|y\rangle$ quantum coherence is observable and whose oscillating character comes from the $|x\rangle/|y\rangle$ energy splitting.

Figure 4 shows the dynamical dichroism decay curves

obtained for a circular and for a linear pump beam. In the case of a linearly polarized pump beam, a spurious small signal of linear dichroism is superimposed onto a damped cosine function; this unwanted effect is attributed to an experimental misalignment of the x and y sample axes with respect to the experimental setup axes.³¹ For the case of a circularly polarized pump beam, the signal-vs-delay curve clearly shows a damped sine oscillation. Fits of these two curves to cosine or sine damped functions, following Eqs. (9b) and (9c), give a period of $100\pm 20\ \text{ps}$, from which we deduce the mean energy splitting $\hbar\delta_1=41\pm 8\ \mu\text{eV}$ between the linear e - h pair states. These fitting curves also give a lower limit to the value of the decoherence time for a QD: $T_2^*=16\ \text{ps}$. This value, very small as compared to the radiative lifetime (around 1 ns), is likely to result from a wide distribution of the energy splitting $\hbar\delta_1$ over the collection of measured QDs, this distribution including possibly positive and negative energy splittings (the assumption of a Gaussian distribution only weakly reduces the width of the dispersion on $\hbar\delta_1$, without improving the fits, and conserving the main conclusion of its wide distribution among the QDs). Our results are consistent with time-resolved PL measurements performed on the same sample,¹⁵ which yield $\hbar\delta_1=30\pm 3\ \mu\text{eV}$ and $T_2^*=30\ \text{ps}$. They are also comparable to $T_2^*=58\ \text{ps}$ and $\hbar\delta_1=40\ \mu\text{eV}$ obtained by Lenihan *et al.*¹² Recently, Tartakovskii *et al.*¹⁷ have obtained, at 10 K, in self-assembled InGaAs QDs presenting a very narrow distribution of fine-structure splitting energies, a decoherence time of 400 ps, comparable to the lifetime.

VI. CONCLUSION

In conclusion, the dynamics of the photoinduced linear dichroism of our InAs QDs, studied under strictly resonant conditions, is consistent with a very long spin-flip time, as compared to the radiative time; it gives two different population lifetimes of mean value 1.1 ns, arising from two different oscillator strengths for the Π_x and Π_y transitions, which are in the ratio $r=0.88\pm 0.02$. In addition, dynamical dichroism experiments provide a measurement of the fine-structure splitting of the e - h pair states, which is found to be $41\pm 8\ \mu\text{eV}$ at 1.343 eV, and fix a minimum value to the spin decoherence time of about 16 ps. We developed a simple model of our pump-probe measurements, describing very satisfactorily our experimental results. In order to reveal the spin decoherence in InAs QDs, experiments measuring the dynamical dichroism of a single QD would be very interesting.

ACKNOWLEDGMENTS

This work was supported by the Research Ministry through an ‘‘ACI Jeunes Chercheurs 2002’’ grant and by the Île-de-France Regional Council through the ‘‘projet SESAME 2003’’ No. E.1751.

APPENDIX A

To measure the temporal evolution of the QDs after the pump pulse excitation, the probe pulse is sent to the out-of-

equilibrium sample at a time delayed from the arrival of the pump pulse; this variable pump-probe delay is denoted Δt . As shown in the following, for well-chosen polarization configurations of the pump and probe beams, the detection of the probe pulse after its interaction with the QDs reveals their (averaged) quantum state at Δt . The envelopes of the probe field linear components being $e_j(t) = e_{0j} p(t - \Delta t)$ ($j = x, y$) in the $z = 0$ plane, the coupling of the probe with the Π_x and Π_y transitions is characterized by the Rabi frequencies $\omega_{0j} = d_j e_{0j} / \hbar$ ($j = x, y$). In the following, the density matrix describing a single QD while it is interacting with the probe field is denoted $\sigma(t)$, the notation $\rho(t)$ being kept for the free evolution after the pump pulse. The initial condition is $\sigma(t) = \rho(t)$ just before the arrival of the probe pulse on the layer of QDs. The evolution equation for $\sigma(t)$,

$$i\hbar \frac{d\sigma}{dt}(t) = [H_0 + H_I(t), \sigma(t)] \quad (\text{A1})$$

[where now the probe field enters in $H_I(t)$, instead of the pump field; see Eq. (1)], being treated to linear order in the probe field, the coherences of $|x\rangle$ or $|y\rangle$ with the ground state are written:

$$\sigma_{jg}(t) = \tilde{\sigma}_{jg}(t) e^{-i\omega t}, \quad j = x \text{ or } y, \quad (\text{A2})$$

with envelopes

$$\begin{aligned} \tilde{\sigma}_{xg}(t) = & \tilde{\rho}_{xg}(\Delta t) + i\{[\rho_g(\Delta t) - \rho_x(\Delta t)]\omega_{0x} \\ & - \rho_{xy}(\Delta t)\omega_{0y}\} \int_{-\infty}^t dt' p(t' - \Delta t) \end{aligned} \quad (\text{A3a})$$

and

$$\begin{aligned} \tilde{\sigma}_{yg}(t) = & \tilde{\rho}_{yg}(\Delta t) + i\{[\rho_g(\Delta t) - \rho_y(\Delta t)]\omega_{0y} \\ & - \rho_{yx}(\Delta t)\omega_{0x}\} \int_{-\infty}^t dt' p(t' - \Delta t). \end{aligned} \quad (\text{A3b})$$

The expressions of Eqs. (A3) are valid for times t within or very near the time interval $[\Delta t - \tau_p, \Delta t + \tau_p]$ of the probe pulse, for the relaxation to be negligible. Clearly, the weak-probe condition is written $|\omega_{0j}| \tau \ll 1$, which is fulfilled in our experiments. The expression of $\tilde{\sigma}_{xg}(t)$, Eq. (A3a), shows that the $|x\rangle/|g\rangle$ coherence built by the probe pulse comes from two origins: (i) the probe-induced Π_x transition, with initial $|g\rangle$ and $|x\rangle$ populations modified by the pump pulse (term with factor $[\rho_g(\Delta t) - \rho_x(\Delta t)]\omega_{0x}$) (ii) the pump-induced $|x\rangle/|y\rangle$ coherence transferred to $|x\rangle/|g\rangle$ coherence by the probe-induced Π_y transition [term with factor $\rho_{xy}(\Delta t)\omega_{0y}$]. The same kind of processes arise in the creation of $\tilde{\sigma}_{yg}(t)$.

Up to now, we took the usual point of view employed when a classical electromagnetic field is interacting with a quantum system: the field remains unchanged, for it is supposed strong enough to be treated classically, and the quantum evolution of the material system is calculated. However, our goal here is to evaluate the influence of a layer of QDs on the probe field upon transmission. There is a way to achieve this program, even though the electromagnetic field

is not quantized:²⁹ each QD is transformed into a classical object represented by its dipole quantum-mean value, of components

$$\langle \hat{d}_j \rangle(t) = \text{Tr}[\sigma(t) \hat{d}_j] = d_j(\sigma_{jg}(t) + \text{c.c.}), \quad j = x \text{ or } y, \quad (\text{A4})$$

whose the probe-induced part radiates a classical electromagnetic field which is added to the probe field after the sample (i.e., in the half space $z > 0$). The superposition of the individual fields radiated by the ensemble of QDs gives an averaged optical electric field, copropagating with the probe field, which possesses the components

$$\mathcal{E}_j(z > 0, t) = \tilde{\mathcal{E}}_j(z > 0, t) e^{i(kz - \omega t)} + \text{c.c.}, \quad j = x \text{ or } y, \quad (\text{A5})$$

where the envelopes are

$$\tilde{\mathcal{E}}_j(z > 0, t) = iZ(\omega N/2) d_j [\tilde{\sigma}_{jg}(t - nz/c) - \tilde{\rho}_{jg}(\Delta t)]_{\text{av}}; \quad (\text{A6})$$

N is the mean number of QDs per unit surface which are at resonance and $Z = (\mu_0 / \epsilon_0)^{1/2} / n$ is the electromagnetic impedance of the GaAs matrix embedding the $z = 0$ layer of QDs ($k = n\omega/c$). An ensemble average is taken on $\tilde{\sigma}_{jg} - \tilde{\rho}_{jg}(\Delta t)$, involving averages of the populations $\rho_j(t)$, $j = x$ or y [Eq. (3)], and of the coherence $\rho_{yx}(t)$ [Eq. (4)] over the collection of resonant QDs. Finally, the electric field of the probe beam after it has crossed the sample ($z > 0$) possesses the components

$$[e_j(t - nz/c) + \tilde{\mathcal{E}}_j(z > 0, t)] e^{i(kz - \omega t)} + \text{c.c.}, \quad j = x \text{ or } y, \quad (\text{A7})$$

where the envelopes $\tilde{\mathcal{E}}_j(z > 0, t)$ originating from the QDs are given by Eqs. (A6) and (A3).

To conclude this appendix, let us stress that the envelope of the QD-radiated field, $\tilde{\mathcal{E}}_j(z > 0, t)$, is proportional to the part of the $|j\rangle/|g\rangle$ coherence which is due to the probe and then contains all the matrix elements of the density matrix $\rho(\Delta t)$ characterizing the photoinduced dynamics of the QDs [see Eqs. (A3)]—only $\rho_{xg}(\Delta t)$ and $\rho_{yg}(\Delta t)$ are missing.

APPENDIX B

In order to physically interpret the effect of the out-of-equilibrium sample on the polarization of the probe beam, the relation between the classical dipole $\langle \hat{\mathbf{d}} \rangle(t) = \text{Tr}[\sigma(t) \hat{\mathbf{d}}]$ of a QD and the incident probe electric field is diagonalized. Writing $\langle \hat{\mathbf{d}} \rangle(t) = \langle \tilde{\mathbf{d}} \rangle(t) e^{-i\omega t} + \text{c.c.}$, $\langle \tilde{\mathbf{d}} \rangle(t)$ being a slowly varying envelope, Eqs. (A4) and (A3) give the relation between the classical dipole of a QD and the probe field, in the form

$$\langle \tilde{\mathbf{d}} \rangle(t) = \frac{i}{\hbar} \left(\int_{-\infty}^t dt' p(t' - \Delta t) \right) [\mathbf{A}] \mathbf{e}_0, \quad (\text{B1})$$

where the elements of the Hermitian matrix $[\mathbf{A}]$ are

$$A_{xx} = [\rho_g(\Delta t) - \rho_x(\Delta t)]d_x^2, \quad (\text{B2a})$$

$$A_{yy} = [\rho_g(\Delta t) - \rho_y(\Delta t)]d_y^2, \quad (\text{B2b})$$

$$A_{yx} = (A_{xy})^* = -\rho_{yx}(\Delta t)d_x d_y. \quad (\text{B2c})$$

The diagonalization of this relationship gives

$$\langle \tilde{\mathbf{d}} \rangle_{\pm}(t) = \frac{i}{\hbar} \left(\int_{-\infty}^t dt' p[t' - \Delta t] \right) A_{\pm} \mathbf{e}_{0\pm}, \quad (\text{B3})$$

where the eigenvalues

$$A_{\pm} = (A_{xx} + A_{yy})/2 \pm [(A_{xx} - A_{yy})^2/4 + |A_{yx}|^2]^{1/2} \quad (\text{B4a})$$

are associated with the eigenpropagation modes

$$\mathbf{e}_{0+} = \begin{pmatrix} \cos \theta \\ -\sin \theta e^{i\Gamma_{yx}} \end{pmatrix}, \quad \mathbf{e}_{0-} = \begin{pmatrix} \sin \theta e^{-i\Gamma_{yx}} \\ \cos \theta \end{pmatrix}, \quad (\text{B4b})$$

with $\tan 2\theta = 2|A_{yx}|/(A_{xx} - A_{yy})$ ($0 < \theta < \pi/2$) and $\Gamma_{yx} = \text{Arg}[\rho_{yx}(\Delta t)] = \Phi_0 - \delta_1 t$.

Finally, if the complex envelope of the probe is $\mathbf{e}_{0\pm} p(t - nz/c - \Delta t)$ before transmission ($z < 0$), then it becomes

$$\mathbf{e}_{0\pm} \left\{ p(t - nz/c - \Delta t) - A_{\pm} Z(N\omega/2\hbar) \int_{-\infty}^{t-nz/c} dt' p(t' - \Delta t) \right\} \quad (\text{B5})$$

after the layer of QDs ($z > 0$), with no change of the polarization $\mathbf{e}_{0\pm}$: the eigenpropagation modes are differently absorbed by the sample. Thus the probe optical pulse feels a dichroism effect on its $\mathbf{e}_{0\pm}$ components. More precisely, the eigenpropagation modes $\mathbf{e}_{0\pm}$ evolving with time as well as their absorptions A_{\pm} —because of the evolution of the sample density matrix $\rho(\Delta t)$ with delay Δt —we are in fact facing a dynamical dichroism.

-
- ¹J.-Y. Marzin, J.-M. Gérard, A. Izraël, D. Barrier, and G. Bastard, *Phys. Rev. Lett.* **73**, 716 (1994); K. Brunner, G. Abstreiter, G. Böhm, G. Tränkle, and G. Weimann, *ibid.* **73**, 1138 (1994).
- ²H. Drexler, D. Leonard, W. Hansen, J. P. Kotthaus, and P. M. Petroff, *Phys. Rev. Lett.* **73**, 2252 (1994).
- ³S. Kim, H. Mhoseni, M. Erdtmann, E. Michel, C. Jelen, and M. Razeghi, *Appl. Phys. Lett.* **73**, 963 (1998).
- ⁴E. Moreau, I. Robert, J.-M. Gérard, I. Abram, L. Manin, and V. Thierry-Mieg, *Appl. Phys. Lett.* **79**, 2865 (2001); C. Santori, D. Fattal, J. Vuckovic, G. S. Solomon, and Y. Yamamoto, *Nature (London)* **419**, 594 (2002); E. Moreau, I. Robert, L. Manin, V. Thierry-Mieg, J.-M. Gérard, and I. Abram, *Phys. Rev. Lett.* **87**, 183601 (2001).
- ⁵P. Michler, A. Kiraz, C. Becher, W. V. Schoenfeld, P. M. Petroff, Lidong Zhang, E. Hu, and A. Imamoglu, *Science* **290**, 2282 (2000); B. Lounis, H. A. Bechtel, D. Gerion, P. Alivisatos, and W. E. Moerner, *Chem. Phys. Lett.* **329**, 399 (2000).
- ⁶A. Imamoglu, D. D. Awschalom, G. Burkard, D. P. DiVincenzo, D. Loss, M. Sherwin, and A. Small, *Phys. Rev. Lett.* **83**, 4204 (1999).
- ⁷E. Biolatti, R. C. Iotti, P. Zanardi, and F. Rossi, *Phys. Rev. Lett.* **85**, 5647 (2000).
- ⁸M. Bayer, A. Kuther, A. Forchel, A. Gorbunov, V. B. Timofeev, F. Schäfer, J. P. Reithmaier, T. L. Reinecke, and S. N. Walck, *Phys. Rev. Lett.* **82**, 1748 (1999).
- ⁹M. Sugisaki, H. W. Ren, S. V. Nair, K. Nishi, S. Sugou, T. Okuno, and Y. Masumoto, *Phys. Rev. B* **59**, R5300 (1999).
- ¹⁰L. Besombes, K. Kheng, and D. Martrou, *Phys. Rev. Lett.* **85**, 425 (2000).
- ¹¹A. J. Williamson, L. W. Wang, and A. Zunger, *Phys. Rev. B* **62**, 12963 (2000).
- ¹²A. S. Lenihan, M. V. Gurudev Dutt, D. G. Steel, S. Ghosh, and P. K. Bhattacharya, *Phys. Rev. Lett.* **88**, 223601 (2002).
- ¹³A. I. Tartakovskii, M. N. Makhonin, I. R. Sellers, J. Cahill, A. D. Andreev, D. M. Whittaker, J.-P. R. Wells, A. M. Fox, D. J. Mowbray, M. S. Skolnick, K. M. Groom, M. J. Steer, H. Y. Liu, and M. Hopkinson, *Phys. Rev. B* **70**, 193303 (2004).
- ¹⁴W. Langbein, P. Borri, U. Woggon, V. Stavarache, D. Reuter, and A. D. Wieck, *Phys. Rev. B* **69**, 161301(R) (2004).
- ¹⁵M. Sénès, B. Urbaszek, X. Marie, T. Amand, J. Tribollet, F. Bernardot, C. Testelin, M. Chamorro, and J.-M. Gérard, *Phys. Rev. B* **71**, 115334 (2005).
- ¹⁶T. Flissikowski, A. Hundt, M. Lowisch, M. Rabe, and F. Henneberger, *Phys. Rev. Lett.* **86**, 3172 (2001).
- ¹⁷A. I. Tartakovskii, J. Cahill, M. N. Makhonin, D. M. Whittaker, J. P. R. Wells, A. M. Fox, D. J. Mowbray, M. S. Skolnick, K. M. Groom, M. J. Steer, and M. Hopkinson, *Phys. Rev. Lett.* **93**, 057401 (2004).
- ¹⁸W. Langbein, P. Borri, U. Woggon, V. Stavarache, D. Reuter, and A. D. Wieck, *Phys. Rev. B* **70**, 033301 (2004).
- ¹⁹J. Tribollet, L. Maingault, A. Lemaître, B. Sermage, J.-M. Gérard, F. Bernardot, C. Testelin, and M. Chamorro, *Phys. Status Solidi C* **1** (3), 585 (2004).
- ²⁰J. Tribollet, F. Bernardot, M. Menant, G. Karczewski, C. Testelin, and M. Chamorro, *Phys. Rev. B* **68**, 235316 (2003).
- ²¹See, e.g., M. O. Scully and M. S. Zubairy, *Quantum Optics* (Cambridge University Press, Cambridge, England, 1997).
- ²²C. Hermann and C. Weisbuch, *Phys. Rev. B* **15**, 823 (1977).
- ²³Our d_j estimate appears to be of the same order of magnitude (25% larger) as that which can be deduced from the oscillator strength measurement and estimate made by R. J. Warburton, C. S. Dürr, K. Karrai, J. P. Kotthaus, G. Medeiros-Ribeiro, and P. M. Petroff, *Phys. Rev. Lett.* **79**, 5282 (1997).
- ²⁴See, e.g., P. L. Knight and L. Allen, *Concepts of Quantum Optics* (Pergamon Press, New York, 1983).
- ²⁵M. Paillard, X. Marie, P. Renucci, T. Amand, A. Jbeli, and J.-M. Gérard, *Phys. Rev. Lett.* **86**, 1634 (2001). [This situation contrasts with the case of nonresonant excitation, where a short spin relaxation time is observed: V. K. Kalevich, M. Paillard, K. V. Kavokin, X. Marie, A. R. Kovsh, T. Amand, A. E. Zhukov, Yu.

- G. Musikhin, V. M. Ustinov, E. Vanelle, and B. P. Zakharchenya, *Phys. Rev. B* **64**, 045309 (2001); see also Ref. 26.]
- ²⁶I. Favero, G. Cassabois, C. Voisin, C. Delalande, P. Roussignol, R. Ferreira, C. Couteau, J.-P. Poizat, and J.-M. Gérard, *Phys. Rev. B* **71**, 233304 (2005).
- ²⁷J. M. Smith, P. A. Dalgarno, R. J. Warburton, A. O. Govorov, K. Karrai, B. D. Gerardot, and P. M. Petroff, *Phys. Rev. Lett.* **94**, 197402 (2005).
- ²⁸P. Borri, W. Langbein, S. Schneider, U. Woggon, R. L. Sellin, D. Ouyang, and D. Bimberg, *Phys. Rev. Lett.* **87**, 157401 (2001); D. Birkedal, K. Leosson, and J. M. Hvam, *ibid.* **87**, 227401 (2001).
- ²⁹Y. R. Shen, *The Principles of Nonlinear Optics* (Wiley, New York, 1984), Chap. 21; E. T. Jaynes and F. W. Cummings, *Proc. IEEE* **51**, 89 (1963). This procedure misses the spontaneous emission of the QDs, which is of no consequence here because it is supposed to be negligible during their interaction with the probe pulse.
- ³⁰In other InAs QDs, the *e-h* second-excited states have already shown a decay time one order of magnitude smaller than the first-excited states: S. Hinooda, S. Fréchengues, B. Lambert, S. Loualiche, M. Paillard, X. Marie, and T. Amand, *Appl. Phys. Lett.* **75**, 3530 (1999).
- ³¹We are confirmed in this view by the complete cancellation of the long-time signal in other experimental runs, performed on the same sample.